Investigation on acoustic reception pathways in finless porpoise *(Neophocaena asiaorientalis sunameri)* with insight into an alternative pathway

Zhongchang Song[1, 2], Yu Zhang[1, 3]*, T Aran Mooney[2], Xianyan Wang[4]*, Adam B Smith[2], Xiaohui Xu[1]

[1]Key Laboratory of Underwater Acoustic Communication and Marine Information Technology of the Ministry of Education, College of Ocean and Earth Sciences, Xiamen University, Xiamen 361005, People's Republic of China

[2]Biology Department, Woods Hole Oceanographic Institution, Woods Hole, MA 02543, USA

[3]Department of Mechanical Engineering, Massachusetts Institute of Technology, Cambridge 02139, MA, USA

[4]Laboratory of Marine Biology and Ecology, Third Institute of Oceanography, State Oceanic Administration, Xiamen 361005, People's Republic of China

*Email: yuzhang@xmu.edu.cn; wangxianyan@tio.org.cn

Abstract

Sound transmission and reception are both vital components to odontocete echolocation and daily life. Here, we combine computed tomography (CT) scanning and Finite Element Modeling to investigate the acoustic propagation of finless porpoise *(Neophocaena asiaorientalis sunameri)* echolocation pulses. The CT scanning and FEM wave propagation model results support the well-accepted jaw-hearing pathway hypothesis and suggest an additional alternative auditory pathway composed of structures, mandible (lower jaw) and internal mandibular fat, with different acoustic impedances, which may also conduct sounds to the ear complexes. The internal mandibular fat is attached to the ear complex and encased by the mandibles laterally and anteriorly. The simulations show signals in this pathway initially propagate along the solid mandibles and are transmitted to the acoustically coupled soft tissue of the internal mandibular fat which conducts the stimuli posteriorly as it eventually arrives at ear complexes. While supporting traditional theories, this new bone-tissue-conduction pathway might be meaningful to understand the hearing and sound reception processes in a wide variety of odontocetes species.

Key Words: Finless porpoise; Reception pathway; Acoustic propagation; Finite element method

PACS: 43.80 Ka

1. Introduction

Odontocetes have a remarkable capability to actively control produced sounds (Au 1993, Au and Hasting 2008). This ability stems from their complex sound production and beam formation systems, which involve different sets of anatomical structures including the solid skull, fluid air components and soft tissues (Aroyan *et al* 1992, Cranford *et al* 1996, Song *et al* 2016, 2017b, Wei *et al* 2017, Zhang *et al* 2017). The combination of these structures forms a natural acoustic material, which provides a gradient of sound speeds and densities to efficiently influence echolocation beam formation (e.g., Zhang *et al* 2017). Bats are often compared to odontocetes with respect to their echolocation abilities (Au 1993, Au and Hasting 2008, Thomas *et al* 2004, Popper and Fay 1995). Despite their body size and the different acoustic properties of the media in which they live (air versus water), these animals have much in common, with both utilizing several separate components to control the propagation and beam formation of projected signals. Some bats have a lancet, sella and anterior leaf in its sound transmission system, which all play roles in beam formation (Zhuang and Muller 2006). In odontocetes, there are skull structures, air components and soft tissues to help form efficient sound beams to detect targets (Thomas *et al* 2004, Aroyan *et al* 1992, Song *et al* 2016, Wei *et al* 2017, Zhang *et al* 2017). The transmission systems of these two taxa both consist of several components with different anatomy and acoustic properties.

With respect to hearing, bats have a set of distinct pinna (outer ear) and tragus (skin in front of ear canal) to conduct sounds into the middle and inner ears for further analysis (Popper and Fay 1995). As for odontocetes, they have developed unique pathways and complex auditory anatomical structures for sound reception (McCormick *et al* 1970, Brill *et al* 1988a, 1988b, 1991, 2001, Møhl *et al* 1999, Norris *et al*, 1961, 1964, 1968, 1969, Norris and Harvey 1974, Ketten 2000, Aroyan 2001). Sounds enter the ear complex via the external mandibular fat pad lying between the skin and posterior lower jaw. Sound is thought to then traverse the jaw thorough a thin portion of bone called the pan-bone. Afterwards, it is conducted into the internal mandibular fat before reaching the tympano-periotic complex. This “jaw hearing” theory was first proposed by Norris (Norris 1964, 1968) and supported in later psychoacoustic and modeling experiments (Brill *et al* 1988a, 1991, Møhl *et al* 1999, Bullock *et al* 1968). This theory is reasonable from an acoustic impedance matching perspective. Soft tissues are distributed extensively within the odontocetes body. The fat body of the mandible has an acoustic impedance close to water (Varanasi and Malins 1970, Song *et al* 2015, 2017a, Wei *et al* 2017). As sound will be refracted towards low sound speed media, this probably helps explain, to some extent, how sound is directed toward the bulla complex from mandibular fat (Norris1968).

Previous studies have raised suggestions of additional modes of odontocete sound reception (Purves 1966, Purves and Pilleri 1983, Cranford *et al* 2008a, 2008b, Goodson and Klinowska 1990). The external auditory meatus was once thought as a route for signals to reach the ear, especially for low frequency sounds (Purves and Pilleri 1983, Renaud and Popper 1975, Popov and Supin 1990). But this was challenged in

physiological, anatomical and behavioral studies (McCormick *et al* 1970, Brill *et al* 1988b, 1991, Møhl *et al* 1999), which showed the external auditory meatus might be vestigial and lower jaw region was important for sound reception. New ideas in sound reception theory and new information for sounds reception pathways have arisen in recent years (Mooney *et al* 2008, 2014, Cranford *et al* 2008b). Cranford *et al* (2008b) refined the notion of jaw hearing theory and proposed a "gular pathway", which describes sounds enter the internal mandibular fat channel through the ventral margin of the mandible in a Cuvier's beaked whale (*Ziphius cavirostris*). Mooney *et al* (2008) stated that there might be acoustic channels beginning at the tip of the rostrum for a beluga whale (*Delphinapterus leucas*) when they measured a good hearing sensitivity at this region. Relative high hearing sensitivities on lower jaw tip were also reported in Risso's dolphins (*Grampus griseus*) and a Yangtze River finless porpoise (*Neophocaena phocaenoides asiaeorientalis*) (Mooney *et al* 2015, Mooney *et al* 2014). Even the teeth overlying the lower jaw are considered as a periodic structures system to play roles in sound reception of the odontocetes and as a passive resonator system (Goodson and Klinowska 1990, Dible *et al* 2009, Dobbins 2007, Graf *et al* 2008). These studies broaden our view of sound reception in odontocetes as well as raise new points for additional research. Though the jaw hearing theory and gular pathway theories seem to be widely accepted in odontocetes hearing regardless of the species difference, much work remains to be done to explain issues e.g. why the hearing sensitivity is high at the tip of the rostrum in many species (Mooney et al 2008).

Most studies related to odontocetes hearing are presented on delphinids, and only a few focus on finless porpoises (Popov *et al* 2005, Mooney *et al* 2014). Finless porpoises are small odontocetes, distributed in both fresh and marine habitats (Pilleri and Gihr 1972). They produce high frequency echolocation clicks with narrow bandwidths to detect targets (Li *et al* 2007). Their audiogram shape is similar to that of many odontocetes species (Popov *et al* 2005, Mooney *et al* 2008, 2014). The best hearing sensitivity of a Yangtze finless porpoise (*N. a. asiaeorientalis*) was found adjacent to the mandibular fat pad (Mooney *et al* 2014). This area of sensitivity appears similar to many other odontocetes e.g., the bottlenose dolphin (*Tursiops truncatus*) and beluga whale (*D. leucas*). However, the detailed sound propagations inside the head pathways have not been investigated yet for finless porpoises. The goal of this study is to examine sound reception pathways in finless porpoises *(Neophocaena asiaorientalis sunameri)* using computed tomography (CT) scanning and numerical simulation. The resulting finite element models help describe the likely sound reception pathways for this species. The results are meaningful to probe into the sound propagation pathways and roles of mandibular fat bodies and mandible in conducting sounds to the tympano-periotic complex. The target animal is a small odontocetes species and the information here could strengthen the understanding of sound reception pathways in this species and provide reference for the sound reception on other odontocetes.

2. Materials and Methods

2.1 CT scanning, sound speed and density estimates

The specimen was a finless porpoise which stranded in Xiamen waters on March 29, 2016 and was delivered immediately to Radiology Department of Affiliated Zhongshan Hospital of Xiamen University for CT scanning. The cause of death was not determined. CT scanning provides an efficient way to image and subsequently reconstruct the anatomical structures of the porpoise's head and allows the major components of the sound emission and reception systems to be clearly seen (Figure 1).

In this study, we focused on the sound reception pathway of the finless porpoise specimen. The components of the sound reception system are arranged along the ventral portions of the solid skull and are connected with the mandibles. The acoustic fat in this region consists of two general components (external and internal mandibular fats) encasing the posterior mandible, also referred to as the pan bone (shown in Figures 1B-E). The external mandibular fat, pan bone and internal mandibular fat make an "acoustic window," which lies in the posterior parts of the mandible and is thought to be one of the primary routes of sound into the head and ear complexes in odontocetes (Norris 1968, Ridgeway 1999, Bullock *et al* 1968, McCormick *et al* 1970, Møhl *et al* 1999, Cranford *et al* 2008b). The internal fat body fills in the pan bone cavity and extends posteriorly to attach to the ear complexes. We extracted a 2-D XZ sound reception path in axial plane (Figure1A) from the 3-D reconstruction of the porpoise head, shown in Figure 1E, for subsequent numerical simulation. The similar process was repeated in sagittal plane to extract an YZ sound reception path.

From the CT scanning results, we built geometric models of the head and reconstructed the acoustic properties (sound speed and density) of head structures. We obtained the Hounsfield Unit (HU) distribution of the porpoise head and subsequently cut the forehead tissues of the specimen into pieces, similar to what we did in a previous study (Zhang *et al* 2017). For each of the pieces, HU values were measured through CT imaging. We used a set of ultrasound probes to emit broadband sound impulse to travel through the tissue pieces and measured the corresponding travelling time. The thickness of the tissue pieces was used to divide the sound travelling time to obtain the tissue pieces' sound speed. The Archimedes principle was employed to measure each pieces' volume, which was used to divide its mass to determine density. Afterwards, regression analysis was used to find linear relationships between tissue pieces' HU and sound speed, as well as HU and density. The relationships were then combined with CT scanning data of the whole head to reconstruct its sound speed and density distributions (Zhang *et al* 2017). Details of the sound speed and density reconstruction could be found in our previous studies (Zhang *et al* 2017, Song *et al* 2015, 2017b).

2.2 Geometric models and numerical simulations

The CT data were used to build the geometrical models of the sound reception system in both the XZ and YZ sections (Figure 2). The sound speed and density settings of soft tissues in the models strictly followed the reconstructions. The sound speeds and densities for water and air were set as 1500 m/s and 998 kg/m^3, 343 m/s and 1.21 kg/m^3, respectively. The density, compressional wave speed and shear wave speed of the solid skull structures followed previous studies (Dible *et al* 2009, Dobbins 2008, Graf *et al* 2007).

We first examined the wave propagations and acoustic fields initiated from five sound source locations (*a, b, c, d, e*) outside the porpoise head in both the XZ and YZ planes (Figure 2). The point "*h*" (located at the mouth) was set as a reference point. The distances between "*h*" and the sound sources were kept at 0.3 m, resulting in incident angles of -30°, -15°, 0°, 15°, and 30° for sound source locations at *a, b, c, d*, and *e*, respectively. The sound propagation from the peripheral water into the head was examined. We placed reception points R1 and R2 in XZ section and R in YZ section in the internal mandibular fat, right anterior to the ear complexes. Using sounds originating from each of the 5 source locations, the received signals at R1 and R2 were compared.

Numerical computations were presented in the time domain. A short duration pulse with the following formula was used for all sound-source excitations:

$$Q_m = A_0 e^{\alpha_0 t} \sin 2\pi f_0 t \qquad 0 \le t \le t_0 \qquad (1)$$

$$Q_m = A_1 e^{(-\alpha_1 t + \alpha_2 t_1)} \sin 2\pi f_0 t \qquad t_0 \le t \le t_{end} \qquad (2)$$

,

where A_0 and A_1 are signal amplitudes, α_0, α_1, and α_2 are the attenuation parameters to control the bandwidth of the pulse, and f_0 is peak frequency of the signal. The variable t is the time variable, with t_0 quantitatively expressing the time from signal onset to peak amplitude, and t_{end} is the terminal time of the signal and describes time from the signal peak amplitude to the end. And t_1 is used as a time offset control to make pulse signal continuous at t_0. The f_0 was set as 125 kHz. α_0, α_1, and α_2 were the same, set as 38000. t_1 was $1/f_0$*11. A_0 and A_1 were both set as 1, to represent normalized pressure. The characteristics of this source signal follow statistical analysis of *in situ* signal recordings of the species which have been reported in previous work (Song *et al* 2017c, Zhang *et al* 2017).

The Finite Element Method (FEM) was used to numerically solve the wave propagation problems. To meet the computing requirements, the numerical models in Figure 2 were meshed into small size elements one-tenth of the wavelength of the sound waves travelling in the media. After sounds were excited at the source, the wave propagations in the models followed the pre-set acoustic equations, which can be found in our previous studies (Song *et al* 2016, 2017b, Zhang *et al* 2017). All soft tissues and air components were modeled as fluids, and bony structures were treated as solids in which the shear waves and compressional waves were both considered. The equations to describe the sound propagations within the solid and fluid medium are different (Song *et al* 2016, Zhang *et al* 2017, Dible *et al* 2009, Cranford and Krysl 2015).

3. Results

3.1 Sound speed and density reconstructions

The sound speed and density results of the chosen XZ planes (axial section) are given in Figure 3A and 3B, respectively, which suggest that the sound speed and density

of the mandibular fat are lower than muscle and connective tissues. We also examined the sound reception process in the YZ section (the sagittal section). Three different planes in the YZ section were extracted and their sound speed and density distributions were estimated (Figures 4B-G). The sound speed and density distributions of the midline plane (YZ plane 1), shown in Figures 4B and 4E, provide a way to view the sound transmission system of the forehead.

In YZ section, the auditory bulla are located in plane 2 and plane 3 (Figure 4A). The sound speed distributions of these two sections are shown in Figures 4C and 4D, and their density distributions are given in Figures 4F and 4G. To provide an initial glimpse into the jaw hearing theory conduction pathways within the head, we mapped the process in a XZ plane, shown in Figures 3C. Incoming sound waves enter the odontocete head through the external mandibular fat, then traverses the pan bone and propagate along the internal mandibular fat body before causing the ear bones to vibrate.

3.2. Simulation in the axial section (XZ section)

The sound reception system along the ventral portion of the finless porpoise head couples structures with different acoustic impedance into a reception pathway. The simulations began in the XZ plane by placing the sound source at a 0° orientation to the head (Point *c*, Figure 2A). We modeled the sound source emitting an omnidirectional sound pulse outside the head at point c and the resulting acoustic fields at four different time points t_1 0.06 ms, t_2 0.16 ms, t_3 0.2 ms, and t_4 0.24 ms are shown in Figure 5. At time t_2 0.16 ms, sound waves reached the head. To better examine these effects we highlighted the sound propagation details at times t_2, t_3 and t_4, shown respectively in the lower part of Figure 5.

When sounds originated from directly in front of the animal, the presence of the mandible and internal mandibular fat created a waveguide for sounds to travel to the ear complexes. Inside the head, the sounds caused vibration and displacement in the solid mandible and then the mandible led sounds along the pellucid fat within the internal cavity of the lower jaw, before reaching the ear complexes.

Additional simulations examined the effect of sounds emitted from incident angles from -30° to 30° (Figure 6), which created different sound fields within the mandible and adjacent tissues. These simulations further verified the sound reception pathway described above regardless of the sound incoming directions. The mandible and internal mandibular fat formed a channel for sounds to propagate to the ear complexes in all these cases. Two series of waves propagated along the external and internal mandibular fat from all incident directions. A portion of the sound was laterally reflected back by the mandible. As the incident angle changed from -15° to -30° the reflection caused by the mandible become greater (Figures 6A and 6B). A similar effect was seen when sounds were emitted by sources located at 15° and 30° (Figures 6C and 6D).

3.3. Simulation in the sagittal section (YZ section)

Simulations were also run in the YZ section. Figure 7 illustrates sound fields at times t_1 0.06 ms, t_2 0.16 ms, t_3 0.2 ms, and t_4 0.24 ms. In this case, the sound source incident angle was 0°. The details of sound propagation at times t_2 0.16 ms, t_3 0.2 ms,

and t_4 0.24 ms are enlarged and shown in lower part of Figure 7. The details showed that the pathway formed by mandible and internal mandibular fat also held true in this plane. The sounds which propagate to the porpoise's head would induce waves in the mandible. These waves then propagated along the internal mandibular fat to the ear complexes. The series of sound waves utilizing the pathway were depicted by the arrow 1 at propagation times t_3 and t_4. The sound propagations at times t_3 0.2 ms, and t_4 0.24 ms showed another series of sound wave, indicated by arrow 2, which supported the jaw hearing theory and "gular" way (Cranford *et al* 2008b). After entering the head through external mandibular fat, the modeled click traversed the jaw and reached the internal mandibular fat on the way to the ear complex (Figure 7).

The simulation in this plane was extended to additional cases with sound source placed at incident angles from -30°to 30° (Figure 8). A look into sound propagations at time t_3 of the cases with sound incident angles of -30°, and -15° suggested that when sound came from these sources, the primary pathway for sounds to enter ear complexes appeared to be within the external mandibular fat, jaw and internal mandibular fat, locations and modalities which have been described in the "jaw hearing" and "gular pathway" theories. However, as sound sources were moved upward, above the horizontal in cases with incident angles of 15°, and 30° respectively, the propagation fields at time t_3 (Figures 8C and 8D) showed the pathway formed by mandible and internal mandibular fat was the dominating one. The results here suggest more than one pathway for sounds to enter the ear complexes.

We analyzed the signal pressures at reception points R1, R2 in XZ plane and R in YZ plane (Figure 2). The sound pressure amplitude arriving at the reception points R1, R2 and R are shown in Figures 9A, 9B and 9C respectively. In Figure 9A, the sound pressures at reception point R1 in XZ plane from sound sources -30°, -15°, 0°, 15°, and 30° are given at *a, b, c, d*, and *e* respectively. The histogram distribution in Figure 9A gives the normalization of highest sound pressure amplitude of the signals from these points. Figures 9B and 9C show the similar signal information for reception points R2 in XZ plane and R in YZ plane. In XZ plane, the sound pressure arriving at the reception point R1 has a highest amplitude from 30° and the highest pressure amplitude at reception point R2 comes from -30°. In XZ plane, sounds emitted from locations on the side of the head caused higher sound pressure amplitudes in the ipsilateral ear than those in the contra-lateral ones. In YZ plane, sounds emitted from -15° lead to the highest pressure amplitude. Figure 9 helps us to understand that sounds outside the head always have a pathway to reach the ear complexes but the pathway efficiency is different.

4. Discussion

The results reveal that the auditory system of the finless porpoise is composed of multiple structures with different acoustic impedances, including solid skull and soft tissues, to form a waveguide for sounds to enter the ear complexes (Figures 1, 3 and 4). The impedance differences between the structures can lead to sound refraction and reflection during sound propagation but more importantly, form a sound channel. The acoustic impedance match between the acoustic fat and water is considered as an

important factor for sounds to propagate with low attenuations (Varanasi and Malins 1970), and likely makes the mandibular fat a preferential path for sounds entering the odontocete head. The internal and external mandibular fat have similar sound speeds and densities. However, greater effort could address their inherent distinctions, e.g., their lipid compositions and carbon contents (Litchfield *et al* 1973), which might help to build a better understanding on the organizations of the fats.

We combined CT scanning with numerical simulation methods to investigate the hearing pathways in finless porpoise. The data and resulting models can potentially be used as a comparative reference for other odontocetes. The simulations shown in Figures 5, 6, 7 and 8 corroborate the "jaw hearing" and subsequent "gular way" theories (Norris 1964, 1968, Cranford *et al* 2008b). More importantly, this study reveals an alternative pathway for sounds to be guided to the ear complexes of the finless porpoise. In this canal, mandible and the fat, which is housed in the mandible cavities play critical roles. Sounds, when reaching the mandible, will initially be conducted along the mandible, then propagate to the internal mandibular fat and finally arrive at the ear complexes. This alternate pathway is a bone-tissue conduction one. The pathway is supplementary for the jaw hearing and gular pathways. In these three pathways, the internal mandibular fat is important due to its adjacency to ear complexes. The difference among these pathways resides at sound entrance to the internal mandibular fat. In jaw hearing, the sounds enter the hearing system from external mandibular fat and then transverses the pan bone to reach internal mandibular fat. The gular pathway uses the soft tissue region at mandible's ventral margin to enter internal mandibular fat. Based on the results in this study, the mandible builds a guide for sounds to reach internal mandibular fat. The mandible plays as a waveguide in the bone-tissue-conduction pathway here. Interestingly, when the sounds are emitted below the horizontal axis in YZ plane, the "jaw hearing" pathway seems to be a primary canal for reception (Figures 8A and 8B). As sound sources are moved to locations above the horizontal (Figures 8C, and 8D), jaw hearing becomes less effective and the pathway described in this paper more efficiently conducts sounds to ear complexes. When sounds were emitted right in front of the head, two pathways both work to guide sounds (Figure 7).

The front portion of the mandibles was found to be the beginning of the potential alternative reception pathway described here. The results might support the auditory evoked potential measurements on a Yangtze river finless porpoise (Mooney *et al* 2014), a beluga whale, (Mooney *et al* 2008), and a Risso's dolphin (Mooney *et al* 2015). These studies demonstrated relatively good hearing sensitivity, and often lower comparable thresholds, at the tips of study animals' rostrums. While the authors ascribe these lower hearing thresholds to hearing responses generated by both ears, an additional hypothesis is that the good hearing sensitivity at rostrum tip might be related to the bone conduction in current paper. In a recent study, Popov *et al* (2016) concluded the sound conduction to the auditory system is frequency dependent. The areas of best sensitivity shifted when the frequency of the acoustic stimuli changed. Generally, the middle parts of lower jaw (mandible) had the best hearing sensitivities. The rostrum tip just showed a relatively high sensitivity for middle-frequency (32 kHz-64 kHz) acoustic stimuli

(Popov *et al* 2016). The simulations here introduced an alternative reception pathway for the target animal, but whether this pathway is responsible for the high hearing sensitivity at the rostrum tips of Beluga whale, Risso's dolphin and Yangtze finless porpoise still needs future studies to address.

The influence of teeth on reception was not examined here. Teeth overlying the mandible have been suggested to function as transducer arrays to create acoustic band gaps for coming sounds and guide sounds in many studies (Goodson and Klinowska 1990, Dible *et al* 2009, Dobbins 2007, Graf *et al* 2008) although this is often debated. These studies extracted and treated teeth as an independent periodic system (Dible *et al* 2009, Graf *et al* 2008). The surrounding tissues and mandible were ignored in their models. When the teeth were treated as an acoustic array, they're similar to photonic crystal system and will form band gaps and passes to control sound propagations (Vasseur et al 2001). But it might be different when regarding them as part of the total odontocete reception system and their roles might be weakened. As stated, there's no establishment to describe the neural links between the teeth arrays and auditory centers (Ketten 2000).

The primary purpose of this work was to model and describe the likely hearing pathways of the finless porpoise. We introduced an additional potential pathway for sounds to reach to ear complexes in this species. Yet it should be noted that the hearing process in this species, and in odontocetes in general, is highly complex and involves more systems as contributors, such as the middle ear, inner ear, cochlea, basilar membrane and neural morphometry (Ketten 2000). For example, the number and size of the cells in cochlea and neural system explains how odontocetes have a wide hearing frequency range (Bullock and Gurevich 1979, Wever *et al* 1971, Ridgeway 1986, Woods *et al* 1986). However, detailed inclusion of all of these contributors is beyond the scope of the work conducted here. Also, a typical narrowband click of the species is used across the directions (Song *et al* 2017c). Normally, the finless porpoises are exposed to various sound signals in their habitants. Future studies might be conducted to use other kinds of signals. The sound source outside the head was set as omnidirectional, which was also an assumption. The real soundscape encasing the animal could be very complicated and sounds could reach the animal in many forms. Whatever the form, the sound pathway disclosed here might still be reliable for various sounds coming to the animal. Though only one animal was used here, the results are potentially applicable to other individuals of this species and some odontocetes species (e.g., other porpoises and some delphinids) given the general similarity of their auditory anatomical systems.

5. Conclusions

The results presented here suggest an alternative pathway for sounds to reach the ear complex that is complementary to the established jaw hearing and gular pathways. This mandible pathway is plausible from perspectives of anatomy and numerical simulation. The CT scanning and reconstructions of the head anatomy reveal the mandibles, internal mandibular fat and ear complexes are organized to compose of a

reliable canal for sounds to propagate. The simulations show the sounds, once entering mandibles, propagate along the mandibles, after which they reach the internal mandibular fat. The sounds then are guided to the ear complexes by the internal mandibular fat.

The results for sound propagation in a porpoise here produce implications for our understanding of hearing in odontocetes. This alternate pathway deserves additional empirical research to verify its reliability. It should also be examined in other odontocetes. Overall, the data reflect that sound is likely received by the head as whole and how it is best conducted and later interpreted can likely be affected by angle of incidence. There may be no signal pathway, rather the head and mandible acts like the tragus of a bat, guiding sound to the bulla complex from many directions. Beyond angle, tested here, sound reception pathways may also be affected by frequency and other signal parameters. As we seek to address how odontocetes use sound for acoustic behaviors, or how they may be impacted by noise, these models can provide an important step towards interpreting the potential impacts or influences of acoustic signals and the overall soundscape in which the animal inhabits.

Acknowledgements

This work is financially supported in part by the National Natural Science Foundation of China (Grants No. 41276040, No. 11174240, and No. 41676023) and the Natural Science Foundation of Fujian Province of China (Grant No. 2012J06010). The Project is also partially sponsored by the Scientific Research Foundation for the Returned Overseas Chinese Scholars, State Education Ministry. The project was sponsored by the Scientific Research Foundation for the Returned Overseas Chinese Scholars, State Education Ministry. The China Scholarship Council financially supports one of the authors, Z. C. Song for his oversea study in Woods Hole Oceanographic Institution. Z. C. Song is also grateful for Ruiqi Li, Shuai Gu, Feng Li, Jie Wang, Weijian Yu, and Shengyao Sun for their support from Xiamen University.

References

Au, W W L 1993 The Sonar of Dolphins (New York: Springer) 277 pp

Au W W L and Hastings M 2008 Principles of Marine Bioacoustics (New York: Springer) pp 65–68

Aroyan J L, Cranford T W, Kent J and Norris K S 1992 Computer modeling of acoustic beam formation in *Delphinus delphis J Acoust. Soc. Am.* 92 2539–45

Aroyan J L 2001 Three-dimensional modeling of hearing in *Delphinus delphis J Acoust. Soc. Am.* 110 3305-18

Brill R L, Sevenich M L, Sullivan T J, Sustman J D, and Witt R E 1988a Behavioral evidence for hearing through the lower jaw by an echolocating dolphin (*Tursiops truncatus*) Mar. Mammal. Sci. 4 223-230

Brill R L 1988b The Jaw-Hearing Dolphin: Preliminary Behavioral and Acoustical Evidence ed P E Nachtigall and P. W. B. Moore (New York: Springer) pp 281-7

Brill R L and Harder P J 1991 The effects of attenuating returning echolocation signals at the lower jaw of a dolphin (*Tursiops truncatus*) *J. Acoust. Soc. Am.* 89 2851–7

Brill R L, Moore P W B, Helweg D A and Dankiewicz L A 2001 *Investigating the Dolphin's Peripheral Hearing System: Acoustic Sensitivity about the Head and Lower Jaw* (San Diego, CA: SPAWAR Systems Center) pp 20

Bullock T H, Grinnell A D, Ikezono E, Kameda K, Katsuki Y, Nomoto M, Sato O, Suga N, and Yanagisaw K 1968 Electrophysiological studies of central auditory mechanisms in cetaceans *J. Comp. Physiol.* 59 117–56

Bullock T H and Gurevich V S 1979 Soviet Literature on the Nervous System and Psychobiology of Cetacea in *International Review of Neurobiology* ed J R Smythies, R J. Bradley (London: Academic Press) pp 47-127

Cranford T W, Amundin M and Norris K S 1996 Functional morphology and homology in the odontocete nasal complex: implications for sound generation *J. Morphol.* 228 223–85

Cranford T W, McKenna M F, Soldevilla M S, Wiggins S M, Goldbogen J A, Shadwick R E, Krysl P, St Leger J A and Hildebrand J A 2008a Anatomic geometry of sound transmission and reception in Cuvier's beaked whale (*Ziphius cavirostris*) *Anat. Record* 291 353-78

Cranford T W, Krysl P and A Hildebrand J A 2008b Acoustic pathways revealed: simulated sound transmission and reception in Cuvier's beaked whale (*Ziphius cavirostris*) *Bioinsp. Biomim.* 3 016001

Cranford T W and Krysl P 2015 Fin Whale Sound Reception Mechanisms: Skull Vibration Enables Low-Frequency Hearing *Plos One*. 10 e0116222

Dible S A, Flint J A and Lepper P A 2009 On the role of periodic structures in the lower jaw of the atlantic bottlenose dolphin (*Tursiops truncatus*) *Bioinsp. Biomim.* 4 015005

Dobbins P F 2007 Dolphin Sonar –Modelling a new receiver concept *Bioinsp. Biomim.* 2 19-29

Goodson A D and Klinowska M 1990 A Proposed Echolocation Receptor for the Bottlenose Dolphin (*Tursiops mincatus*): Modelling the Receive Directivity from Tooth and Lower Jaw Geometry in *Sensory Abilities of Cetaceans* ed Thomas JA and Kastelein R A (New York: Plenum Press) pp 255-67

Graf S, Megill W M, Blondel P and Clift S E 2008 Investigation into the possible role of dolphins' teeth in sound reception *J. Acoust. Soc. Am.* 123 3360

Ketten D R 2000 Cetacean ears Hearing by Whales and Dolphins ed W W L Au, A N Popper and R R Fay (New York: Springer) pp 43–108

Li S H, Wang D, Wang K X, Akamatsu T, Ma Z Q, and Han J B 2007 Echolocation click sounds from wild inshore finless porpoise (*Neophocaena phocaenoides sunameri*) with comparisons to the sonar of riverine *N. p. asiaeorientalis J. Acoust. Soc. Am.*121 3938-46

Litchfield C, Karol R, and Greenberg A 1973 Compositional topography of melon lipids in the Atlantic bottlenosed dolphin *Tursiops truncatus*: Implications for echo-location *Marine Biol.* 23 165–69.

McCormick J G, Wever E G, and Palin J 1970 Sound conduction in the dolphin ear *J. Acoust. Soc. Am.* 48 1418-28

Møhl B, Au W W L, Pawloski J and Nachtigall P E 1999 Dolphin hearing: relative sensitivity as a function of point of application of a contact sound source in the jaw and head region *J. Acoust. Soc. Am.* 105 3421–24

Mooney T A, Nachtigall P E, Castellote M, Taylor K A, Pacini A F and Esteban J A 2008 Hearing

pathways and directional sensitivity of the beluga whale, *Delphinapterus leucas J. Exp. Mar. Biol. Ecol.* 362 108-16

Mooney T A, Li S H, Ketten D R, Wang K X and Wang D 2014 Hearing pathways in the Yangtze finless porpoise, *Neophocaena asiaeorientalis asiaeorientalis J. Exp. Biol.* 217 444-52

Mooney T A, Yang W C, Yu H Y, Ketten D R, and Jen I F 2015 Hearing abilities and sound reception of broadband sounds in an adult Risso's dolphin (Grampus griseus) *J Comp Physiol A.* 201 751–61

Norris K S, Prescott J H, Asa-Dorian P V and Perkins P 1961 An experimental demonstration of echolocation behavior in the porpoise, *Tursiops truncatus* (Montagu) *Biol. Bull.* 120 163–76

Norris, K. S. 1964 Some problems of echolocation in cetaceans in *Marine Bioacoustics*, ed by W. N. Tavolga (New York: Pergamon) pp. 316–36.

Norris K S 1968 The evolution of acoustic mechanisms in odontocete cetaceans in *Evolution and Environment* ed E. T. Drake (New Haven: Yale University Press) pp 297-324

Norris K S 1969 The echolocation of marine mammals *The Biology of Marine Mammals* ed H T Andersen (New York: Academic) pp 391–423

Norris K S and Harvey G W 1974 Sound transmission in the porpoise head *J. Acoust. Soc. Am.* 56 659–64

Pilleri G, and Gihr M 1975 On the taxonomy and ecology of the finless black porpoise, *Neophocaena* (*Cetacea, Delphinidae*) *Mammalia* 39 657–74.

Popov V V and Supin A Y1990 Localization of the Acoustic Window at the Dolphin's Head in *Sensory Abilities of Cetaceans* ed Thomas JA and Kastelein R A (New York: Plenum Press) pp 417-26

Popov V V, Supin A Y, Wang D, Wang K X, Xiao J Q and Li S H 2005 Evoked-potential audiogram of the Yangtze finless porpoise Neophocaena phocaenoides asiaeorientalis (L) *J. Acoust. Soc. Am.* 117, 2728-31

Popov V V, Sysueva E V, Nechaev D I, Lemazina A A, and Supina A Y 2016 Auditory sensitivity to local stimulation of the head surface in a beluga whale (Delphinapterus leucas) *J. Acoust. Soc. Am.* 140, 1218-26

Popper A N and Fay R R 1995 Hearing by Bats (New York: Springer) pp 515

Purves P E 1966 Anatomy and physiology of the outer and middle ear in cetaceans in *Whales, dolphins, and porpoises* ed K S Norris (Berkeley: University of California Press) pp 321-80

Purves P E and Pilleri G E 1983. Echolocation in whales and dolphins (London: Academic Press) pp 631

Renaud D L and Popper A N 1975 Sound localization by the bottlenose porpoise *Tursiops truncatus* J. Exp. Biol. 63 569-85

Ridgeway S H 1999 An illustration of Norris' acoustic window *Mar. Mammal. Sci.* 15(4) 926-930

Ridgeway S H 1986 Physiological observations on dolphin brains in *Dolphin Cognition and Behavior: A Comparative Approach* ed Schusterman R, Thomas J A, Wood F G (Hillsdale:Lawrence Erlbaum Associates) 31-59

Song Z C, Xu X, Dong J C, Xing L R, Zhang M, Liu X C, Zhang Y, Li S H, and Berggren P 2015 Acoustic property reconstruction of a pygmy sperm whale (*Kogia breviceps*) forehead based on computed tomography imaging *J. Acoust. Soc. Am.* 138 3129–37

Song Z C, Zhang Y, Wei C, and Wang X Y 2016 Inducing rostrum interfacial waves by fluid-solid coupling in a Chinese river dolphin (*Lipotes vexillifer*) *Phys. Rev. E* 93, 012411

Song Z C, Zhang Y, Berggren P, and Wei C 2017a Reconstruction of the forehead acoustic properties in an Indo-Pacific humpback dolphin (*Sousa chinensis*), with investigation on the responses of soft tissue sound speed to temperature *J. Acoust. Soc. Am.* 141, 681–89

Song Z C, Zhang Y, Berggren P, and Wei C 2017b The influence of air-filled structures on wave propagation and beam formation of a pygmy sperm whale (*Kogia breviceps*) in horizontal and vertical planes *J. Acoust. Soc. Am.* 142, 2443–53

Song Z C, Zhang Y, Wang X Y, Wei C, Wu F X and Miao X 2017c Vocalizations of a Wild Finless Porpoise (*Neophocaena asiaeorientalis sunmeri*) in the Western Coast of the Taiwan Strait *J. Biobased. Mater. Bi.* 11, 45-52

Thomas J A, Moss C F, and M Vater 2004 Echolocation in bats and dolphins (Chicago and London:The University of Chicago Press) pp 631

Varanasi U S and Malins D C 1970 Ester and ether-linked lipids in the mandibular canal of a porpoise (*Phocoena phocoena*). Occurrence of isovaleric acid in glycerolipids *Biochemistry* 9 4576–79

Vasseur J O, Deymier P A, Chenni B, Djafari-Rouhani B, Dobrzynski L, and Prevost D 2001 Experimental and Theoretical Evidence for the Existence of Absolute Acoustic Band Gaps in Two-Dimensional Solid Phononic Crystals. *Phys Rev Lett* 86 3012-15

Wei C, Wang Z T, Song Z C, Wang K X, Wang D, Au W W L, and Zhang Y 2015 Acoustic property reconstruction of a Yangtze finless porpoise's (*Neophocaena asiaeorientalis*) head base on CT imaging *PLoS One*. 10 e0121442

Wever E G, McCormick J G, Palin J and Ridgeway S H 1971 The Cochlea of the Dolphin, *Tursiops truncatus:* Hair Cells and Ganglion Cells *Proc. Nat. Acad. Sci. USA* 68 2908-12

Woods D L, Ridgeway S H, and Bullock T H 1986 Middle and long latency auditory event related potentials in dolphins in *Dolphin Cognition and Behavior: A Comparative Approach* ed Schusterman R, Thomas J A, Wood F G (Hillsdale:Lawrence Erlbaum Associates) 61-79

Yamato M, Ketten D R, Arruda J, Cramer S, Moore K 2012 The Auditory Anatomy of the Minke Whale (Balaenoptera acutorostrata): A Potential Fatty Sound Reception Pathway in a Baleen Whale *Anat. Record* 295 991–8

Zhang Y, Song Z C, Wang X Y, Cao W W and Au W W L 2017 Directional Acoustic Wave Manipulation by a Porpoise via Multiphase Forehead Structure Phys. Rev. Appl. 8 064002

Zhuang Q and Mulelr R 2006 Noseleaf Furrows in a Horseshoe Bat Act as Resonance Cavities Shaping the Biosonar Beam *Phys. Rev. Lett.* 97 218701

Figure Legends

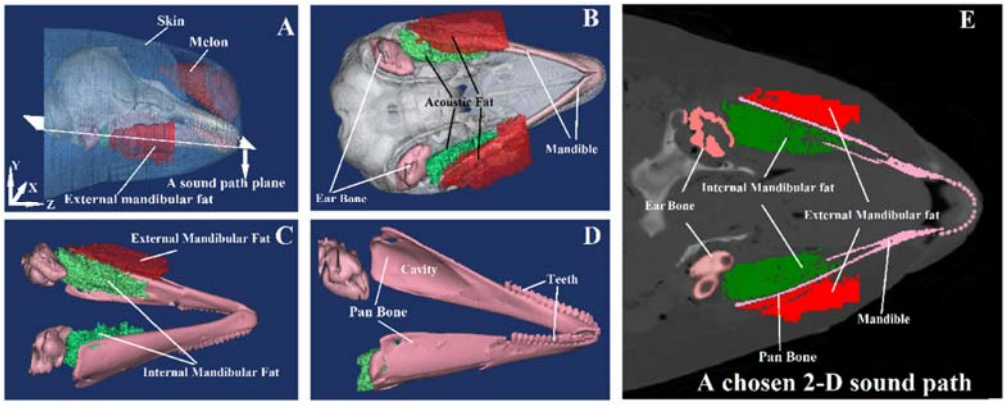

Figure 1 (A) The reconstructed head of the finless porpoise (*N. a. sunameri*) in three dimensions. **(B)** Major components of the biosonar reception system, with ear bone and mandible shown in pink. (C) Acoustic fat includes external mandibular fat (red) and internal mandibular fat (green). (D) The external mandibular fat (red) and internal mandibular fat (green) encase the pan bone, with internal mandibular fat lies in the pan bone cavity. (E) A chosen 2-D sound path of the reception system. Figure 1 provides a frame of the reception system of the species. The internal mandibular fat lies within the cavity of pan bone and attaches to the ear bone. The external mandibular fat overlies the pan bone and extends outward to the skin, while the teeth overlie the mandibles.

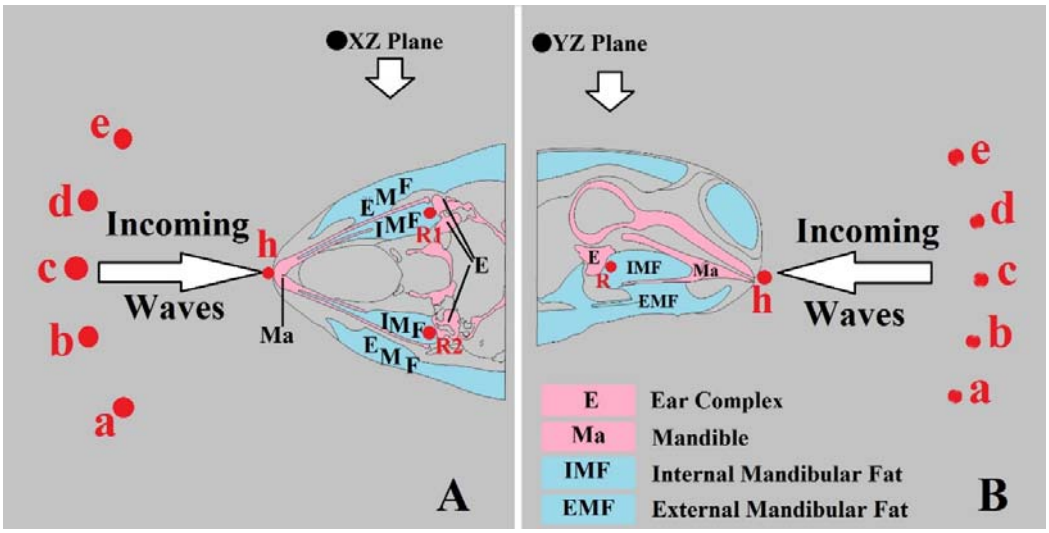

Figure 2 The illustration of the model layouts in the XZ section (A) and YZ section (B), where the major components of the reception system are given. The points outside the head models are set as separate sound sources, with a same distance to the head reference point h as 0.3m. The angles of the points a, b, c, d, and e orienting point h are -30°, -15°, 0°, 15°, and 30°respectively.

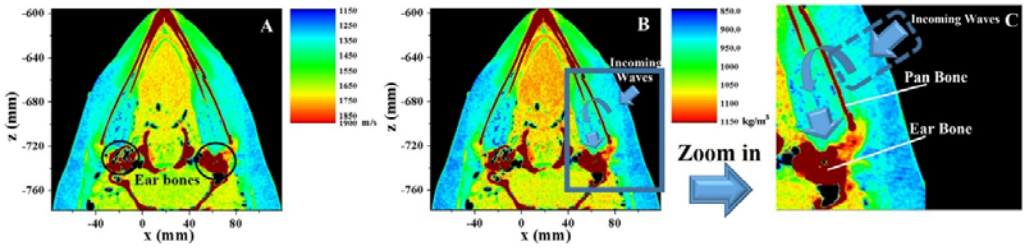

Figure 3 Sound speed (A) and density (B) reconstructions of the porpoise sound reception path in a XZ plane. The distributions clearly suggest the sound speeds and densities are lower in internal and external mandibular fat than in surrounding tissues. The box in B is enlarged and shown in C to give more details of the jaw-hearing pathway for the species. The incoming sound waves enter the porpoise through an "acoustic window" (Norris 1968), transverse the pan bone and propagate along the internal mandibular fat to arrive at the ear complexes.

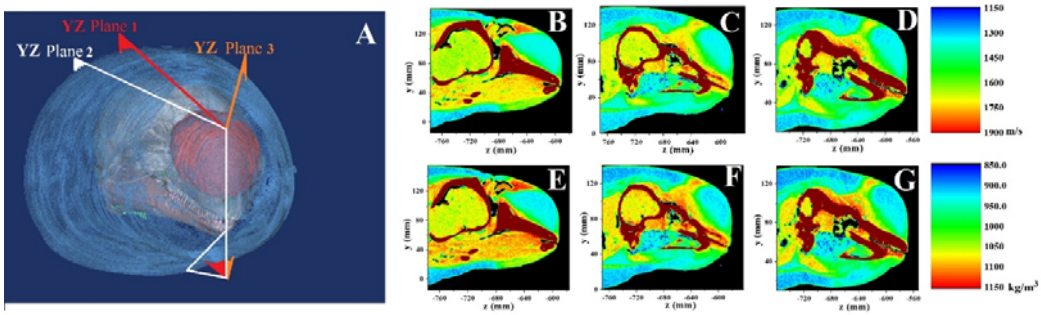

Figure 4 (A) Three YZ planes are denoted. (B) Sound speed distribution of YZ plane 1; (C) Sound speed distribution of YZ plane 2; (D) Sound speed distribution of plane 3; (E) Density distribution of YZ plane 1; (F) Density distribution of YZ plane 2; (G) Density distribution of plane 3; Sound speeds and densities are lower in the forehead core, internal and external mandibular fat than in surrounding tissues.

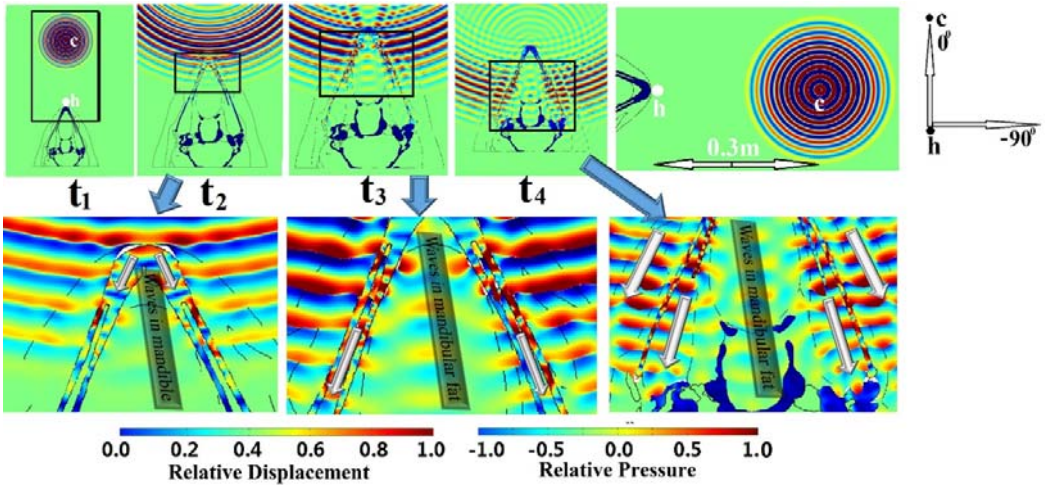

Figure 5 Propagation plots for an omnidirectional short-duration impulse source, with an incident angle of 0° in XZ plane, where t_1, t_2, t_3, and t_4 correspond to the propagation times at 0.06 ms, 0.16 ms, 0.2 ms, and 0.24 ms, respectively. The propagation details at times t_2, t_3, and t_4 are enlarged and shown below. The waves propagate within the mandibles to internal mandibular fat and then are

guided to the ear complexes along the internal mandibular fat. Relative Displacement represents the normalized displacement in the solid mandibles and skull structures; Relative Pressure represents the normalized sound pressure in the fluid tissue. Points c and h represent the sound source and reference point at head, between which the distance is 0.3 m.

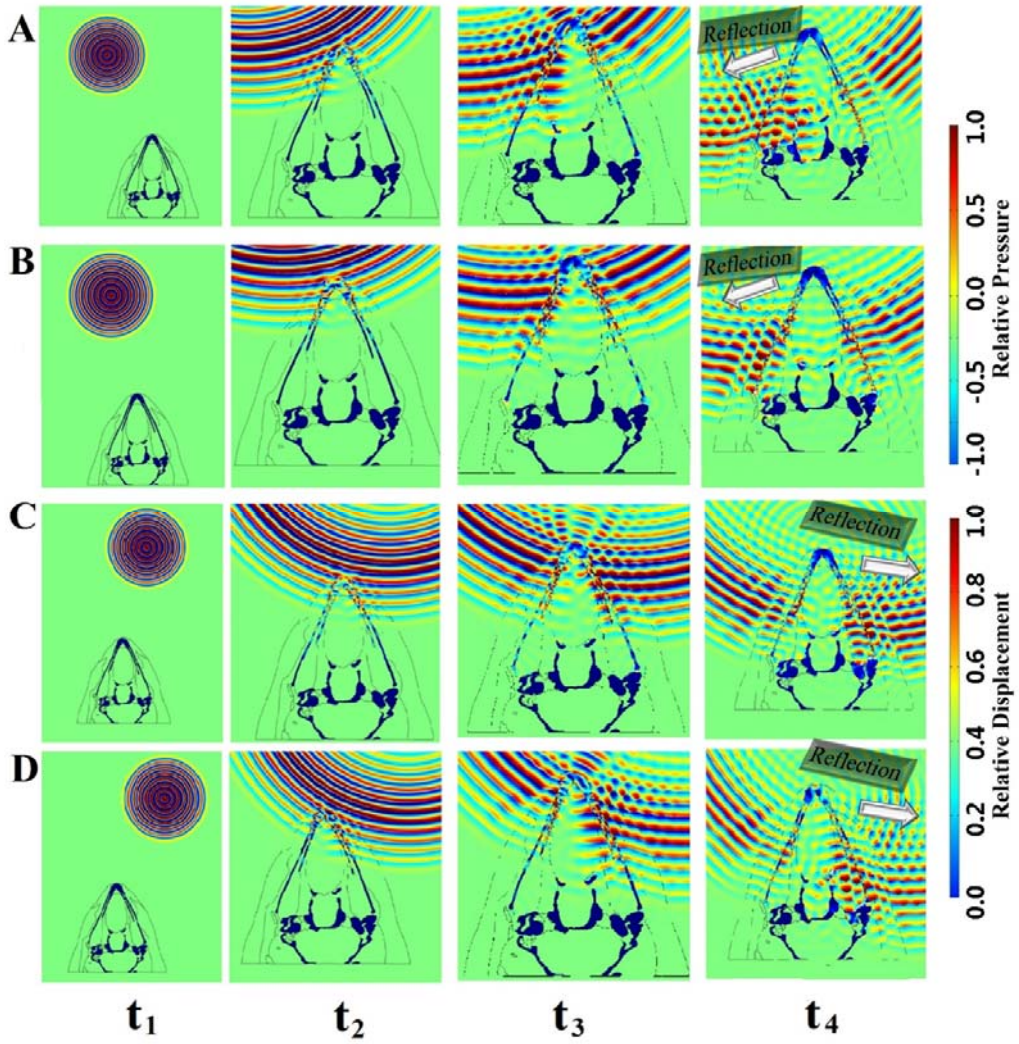

Figure 6 Propagation plots of four omnidirectional short-duration impulse sources in XZ plane, where A, B, C, and D correspond to the cases with different incident angles to the head, with A as -30°, B -15°, C 15°, and D 30° respectively. And t_1, t_2, t_3, and t_4 represent propagation times of 0.06 ms, 0.16 ms, 0.2 ms, and 0.24 ms. The distance between the sources and the head is 0.3 m.

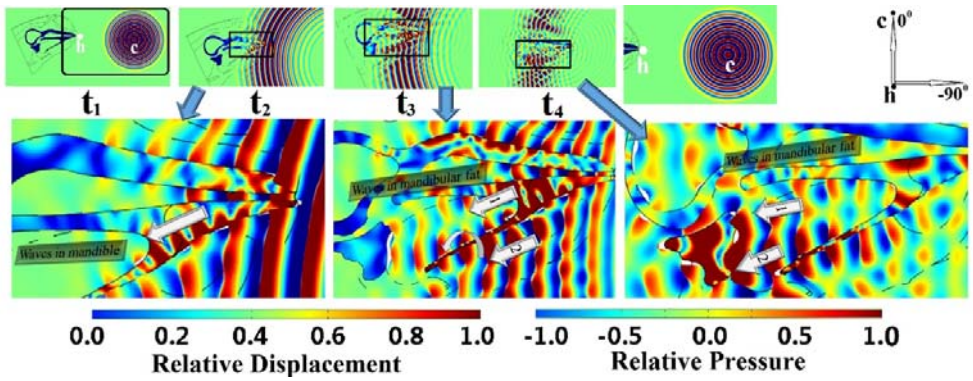

Figure 7 Propagation plots of an omnidirectional short-duration impulse source with an incident angle of 0° in YZ plane, where t_1, t_2, t_3, and t_4 correspond to the propagation times at 0.06 ms, 0.16 ms, 0.2 ms, and 0.24 ms, respectively. The propagation details at times t_2, t_3, and t_4 are enlarged and shown in lower half, where the waves have two separate series to propagate to the ear complexes. A wave series propagates within the mandible and then along the internal mandibular fat, arriving at the ear complexes (Arrow 1). Another sound wave follows the traditional jaw-hearing pathway (Arrow 2), entering the external mandibular fat and transverse the mandible to reach internal mandibular fat, along which the sound waves propagate to the ear complexes. The difference between these two pathways resides at sound entrance to the internal mandibular fat. In an alternative pathway revealed in current paper (Arrow 1), the mandible builds a guide for sounds to reach the internal mandibular fat. In jaw hearing pathway (Arrow 2), the sounds enter the hearing system from external mandibular fat and then transverses the pan bone to reach internal mandibular fat. The distance between points c and h is 0.3 m.

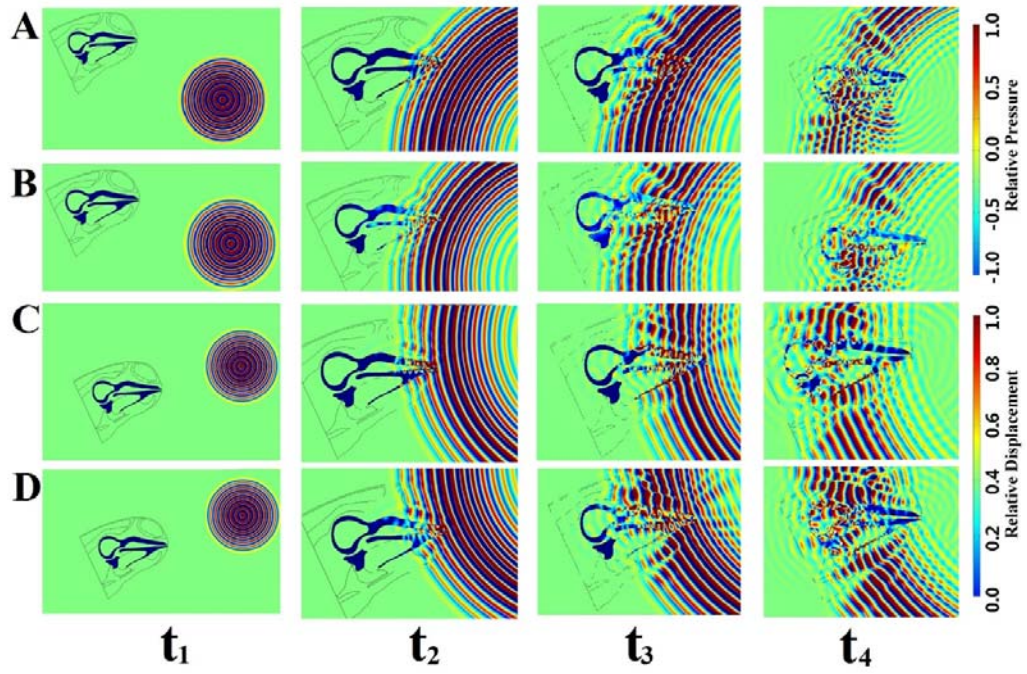

Figure 8 Propagation plots of sound sources emitted from different incident angles -30°, -15°, 15°, and 30° are shown in A, B, C, and D respectively. The propagations at times t_1, t_2, t_3, and t_4 correspond to 0.06 ms, 0.16 ms, 0.2 ms, and 0.24 ms, respectively. The sounds emitted below the

horizontal causes the waves to propagate mainly along the jaw-hearing pathway while those above the horizontal induce the sounds to propagate mainly along the alternative sound pathway. Relative displacement and sound pressure in the solid skull structures and in the fluid tissue are shown by the icons. The distances between sound sources and head are 0.3 m.

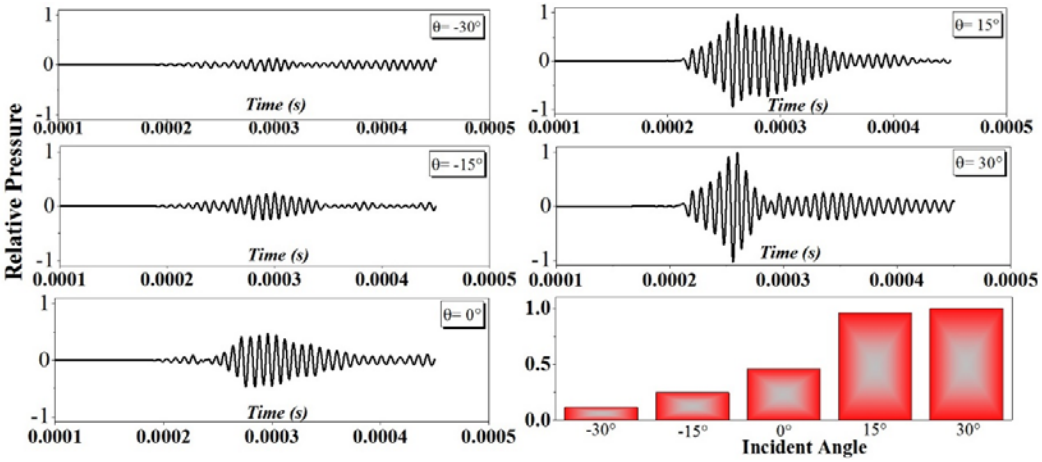

A

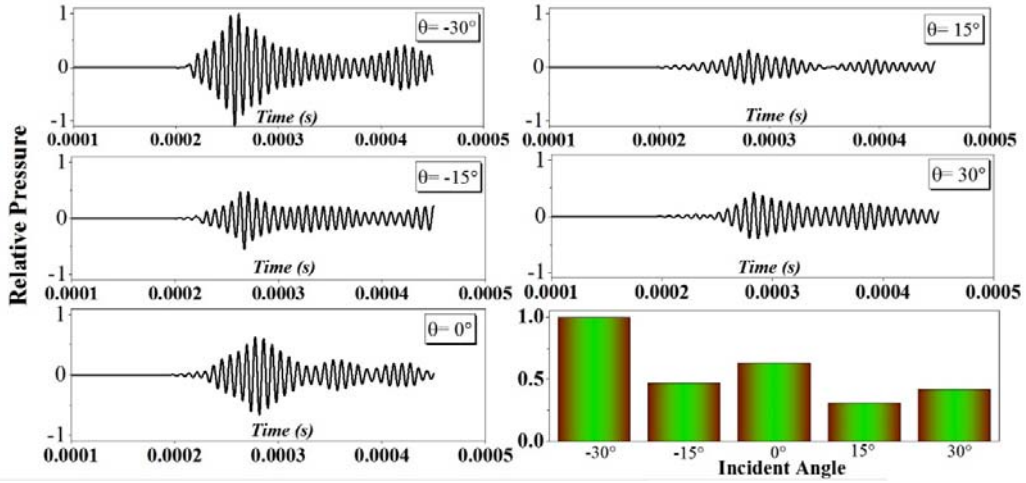

B

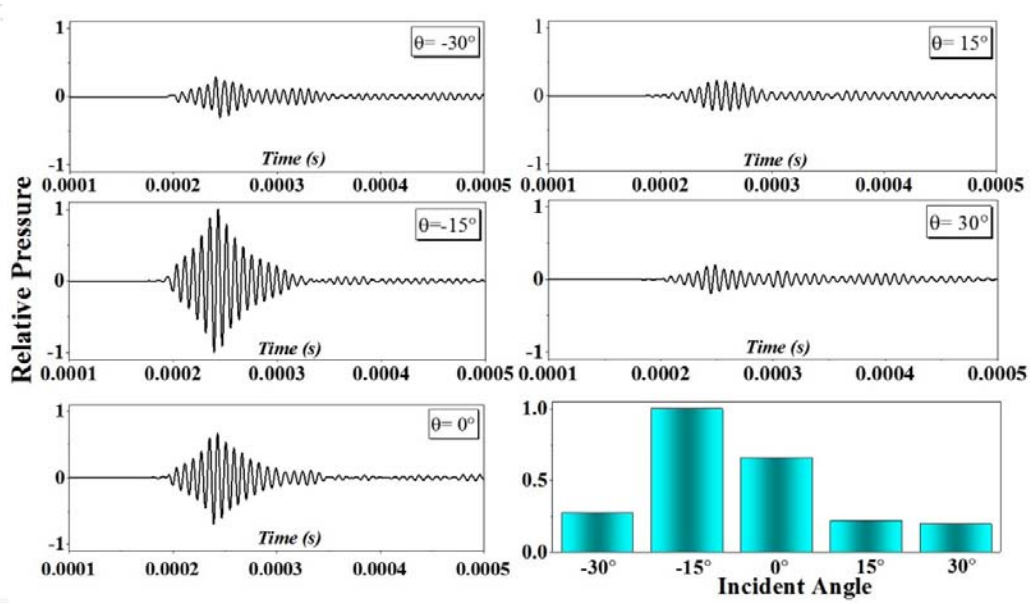

C

Figure 9 This Figure shows the signals arriving at the right ear complex (A) and left ear complex (B) in XZ section, and (C) ear complex in yZ section. In the right ear complex of the XZ section, shown in A, the highest amplitude arrives from 30° and the right sound sources with incident angles of 15° , and 30° induce stronger amplitudes than those of the left ones from -30° , and -15° . In the left ear complex of XZ section, shown in B, the situation is similar. The highest amplitude arrives from -30° . The pressure amplitudes from orientations -30° , and -15° are higher than those from 15° , and 30° . In YZ section, the highest amplitude comes from -15° .